Journal of Photochemistry and Photobiology A: Chemistry 212 (2010) 75–80

Contents lists available at ScienceDirect

Journal of Photochemistry and Photobiology A: Chemistry

journal homepage: www.elsevier.com/locate/jphotochem

Coordination bonding assembly, characterization and photophysical properties of lanthanide (Eu, Tb)/zinc centered hybrid materials through sulfide bridge

Bing Yan*, Xiao-Long Wang, Kai Qian, Hai-Feng Lu

Department of Chemistry, Tongji University, Siping Road 1239, Shanghai 200092, China

ARTICLE INFO

Article history:
Received 1 July 2009
Accepted 29 March 2010
Available online 3 April 2010

Keywords:
Coordination bonding assembly
Sulfide bridge
Hybrid material
Luminescence

ABSTRACT

Two novel molecular sulfide bridges have been achieved through the modification of 4-mercaptobenzoic acid by two crosslinking reagents (3-methacryloyloxypropyl trimethoxysilane, 3-glycidoxypropyltrimethoxysilane). Then six kinds of lanthanide (Eu^{3+}, Tb^{3+})/zinc organic–inorganic hybrid materials through the chemical bonds (coordination bond and covalent bond) have been assembled. All of these hybrid materials exhibit homogeneous microstructures, suggesting the occurrence of self-assembly of the inorganic network and organic units. Especially, the photophysical properties of these hybrid systems are studied in detail, which present three-color luminescence (blue for Zn^{2+}, red for Eu^{3+} and green for Tb^{3+}).

1. Introduction

Organic–inorganic hybrid materials have been attracted great attention because of their extraordinary properties to combine the mutual advantages of both organic and inorganic networks [1–4]. They have great potential values for many applications due to the synergy between the properties of two different building blocks. Generally speaking, the inorganic parts can offer the good mechanical properties and the organic parts can act as functional units [5]. Most of these hybrid materials can be prepared by the sol–gel technology, which derives from the hydrolysis/polycondensation reactions of metal alkoxides and exhibits unique characteristics such as convenience, low temperature and versatility [6–8].

Lanthanide complexes are famous for their special luminescence properties consisting of broad spectral range, strong narrow-width emission band in the visible region, wide range of lifetimes, etc. So in the past few decades, inorganic matrices doped with lanthanide organic complexes have been reported for optical applications owing to their excellent luminescence characteristics [9–11]. Firstly, the conventional doping method is used to synthesize the hybrid materials, unfortunately they are unable to solve the problem of the clustering of emitting centers, inhomogeneous dispersion of the two phases, and leaching of the photoactive molecules for only weak interactions (such as hydrogen bonding, van der Waals forces, or weak static effects) exist between organic and inorganic moieties [12]. Therefore, another appealing method to construct hybrid materials containing chemical bonds has emerged [13,14], which reveals that the possibility of tailoring the complementary properties of novel multifunctional advanced materials can be realized. Franville et al. have concentrated on the modification of pyridine-dicarboxylic acid or their derivatives and resulted in strong Eu^{3+} ions' emissions due to efficient ligand-to-metal energy transfer [15]. Zhang and his co-workers are focused on the modification of the heterocyclic ligands like 1,10-phenanthroline and 2,2′-bipyridyl [16,17]. Carlos and co-workers have prepared hybrids that contain OCH_2CH_2 (polyethylene glycol, PEG) repeated units grafted on to a siliceous backbone by urea (–NHC(=O)NH–), orurethane (–NHC(=O)O–) bridges [18,19]. Our research team has also carried out extensive work in the preparation of molecular hybrids by modifying the amino groups [20,21]; the carboxylate group [22,23]; the hydroxyl groups [24–26]; sulfonic groups [27]; the methylene group [28] of the organic ligands for rare earth ions. After the modification, the above modified bridge ligands can be assembled with lanthanide ions and tetraethoxysilane (TEOS) to compose the chemically bonded hybrid systems.

It is well know that the mercapto group is active in many reactions [28–30]. We also have achieved the modification of the mercapto group of some organic compounds to assemble hybrid materials [31,32]. So in this paper, sulfide bond is selected to construct the linkage between inorganic/organic parts. Two kinds of silane crosslinking reagents, 3-methacryloyloxypropyltrimethoxysilane, 3-glycidoxypropyltrimethoxysilane are chosen to modify the 4-mercaptobenzoic acid to afford to two kinds of molecular bridge. Subsequently, two series of luminescent hybrid molecular-based materials are assembled through chemical bonds via sol–gel process.

* Corresponding author. Tel.: +86 21 65984663; fax: +86 21 65982287.
E-mail address: byan@tongji.edu.cn (B. Yan).

1010-6030/$ – see front matter © 2010 Elsevier B.V. All rights reserved.
doi:10.1016/j.jphotochem.2010.03.011

2. Experimental

2.1. Materials

Starting materials are purchased from Aldrich and are used as received. All organic solvents are purified by common methods before utilization. Tetraethoxysilane (TEOS) is distilled and stored under N_2 atmosphere. Europium and terbium nitrates are prepared by dissolving lanthanide oxides in concentrated nitric acid.

2.2. Synthesis of precursors

Two precursors are prepared according to the procedures in Ref. [31,32] and depicted in Fig. 1, using 4-mercaptobenzoic acid (T) as starting reagent [33]. The modifications are performed by the addition of 3-methacryloyloxypropyl trimethoxysilane (S_1), 3-glycidoxypropyltrimethoxysilane (S_2), respectively.

Modification of 4-mercaptobenzoic acid by 3-methacryloyloxypropyltrimethoxysilane 0.308 g (2 mmol): 4-Mercaptobenzoic acid is first dissolved in 15 mL toluene by stirring and then 0.497 g (2 mmol) 3-methacryloyloxypropyl trimethoxysilane is added to the solution dropwise. The whole mixture is refluxing at 60 °C for 4 h by an addition of three drops of triethylamine as catalyst. After filtration, the solution is then condensed to evaporate the solvent. The residue is dried on a vacuum line and yellow oil is obtained (named as P_1).

Modification of 4-mercaptobenzoic acid by 3-glycidoxypropyltrimethoxysilane 0.308 g (2 mmol): 4-Mercaptobenzoic acid and 0.473 g (2 mmol) 3-glycidoxypropyltrimethoxysilane are dissolved in 15 mL pyridine. The whole mixture is refluxing at 80 °C for 4 h. After being condensed to evaporate the solvent and dried on a vacuum line under argon atmosphere, the solution turns to be yellow oil (named as P_2).

2.3. Synthesis of the hybrid materials

The sol–gel-derived hybrid materials are prepared as follows: 0.5 mmol sulfonamide precursor (P_1 for example) is dissolved in the mixture of 5 mL DMF and 2 mL ethanol by stirring. Then 0.17 mmol $Eu(NO_3)_3{\cdot}6H_2O$ and 1.0 mmol tetraethoxysilane (TEOS) are added into the solution to enhance the sol–gel process. The molar ratio of $Eu(NO_3)_3{\cdot}6H_2O/P_1$/TEOS is 1:3:6. One drop of diluted hydrochloric acid is added to promote hydrolysis reaction. At the beginning of the reaction, the individual hydrolysis of the silylated precursors and TEOS are predominant. After hydrolysis, an appropriate amount of hexamethylene-tetramine is added to adjust the pH value to 6–7 and then the polycondensation reactions take place between hydroxyl groups of both the silylated precursors and TEOS. The resulting mixture is agitated magnetically in a covered Teflon beaker for an hour. After that, it is aged at 60 °C for the gelation in 3 days. The gels are collected and ground as powder materials for the property studies. The europium hybrids can be named as Eu-$M_{1,2}$. When $Eu(NO_3)_3{\cdot}6H_2O$ is replaced by $Tb(NO_3)_3{\cdot}6H_2O$, $Zn(AC)_2{\cdot}2H_2O$ in the reagents, another two series of hybrid materials could be prepared.

2.4. Physical measurement

All measurements are performed under room temperature. Fourier transform infrared (FTIR) spectra are recorded within the 4000–400 cm^{-1} region on an (Nicolet Nexus 912 AO446) infrared spectrophotometer with the KBr pellet technique. Ultraviolet absorption spectra are recorded with an Agilent 8453 spectrophotometer. The X-ray diffraction (XRD) measurements are carried out on powdered samples via a "BRUKER D8" diffractometer (40 mA to 40 kV) using monochromated Cu Kα1 radiation (λ = 1.54 Å) over the 2θ range of 10–70°. Scanning electronic microscope (SEM) images are obtained with a Philps XL-30. UV–vis diffuse reflectance spectra (UV–vis DRS) of dry pressed disk samples are obtained on a Lambda-900 UV–vis spectrophotometer and $BaSO_4$ is used as a reference standard. Luminescence (excitation and emission) spectra of these solid complexes are determined with a RF-5301 spectrophotometer. Luminescence (excitation and emission) spectra of these solid complexes are determined with a RF-5301 spectrophotometer. And the fluorescence decay properties are recorded on an Edinburgh Analytical Instrument.

3. Results and discussion

Fig. 2 shows the FTIR spectra for 4-mercaptobenzoic acid (T), selected precursor (P_2) and the hybrid material (Tb-M_2), respectively. By comparing curve T and P_2, the modification reaction of 4-mercaptobenzoic acid can be evidenced by the vanishing of ν(S–H) at 2554 cm^{-1} and an increase of ν(C–S–C) at 695–655 cm^{-1}. Two adjacent sharp peaks at 2951 cm^{-1} and 2843 cm^{-1} in curves for P_2 are $\nu_{as}(CH_2)$ and $\nu_s(CH_2)$ of the long carbon chain in precursor. This phenomenon can also prove the grafting reaction. The broad peak at 3066–2844 cm^{-1} in curve T is the coupling of two 4-mercaptobenzoic acids' carboxyls and it turns into broad peak of ν(O–H) at 3454 cm^{-1} in curves of P_2. The introduction of the organic groups in the silicate inorganic host which occurs in the hydrolysis and condensation process caused the decrease of other peaks' intensities in the curve of Tb-M_2. The ν(Si–C) vibration located in the 1193 cm^{-1} is consistent with the fact that no (Si–C) bond cleavage occurred during hydrolysis and condensation reactions [20]. The broad absorption band at 1200–1100 cm^{-1} (ν(Si–O–Si)) indicates the formation of siloxane bonds [34]. The ν(O–H) vibration located at 3454 cm^{-1} can be due to the molecule water in the final hybrid material. The coordination reaction between Ln^{3+} ions and the ligands is also clearly shown by infrared spectroscopy. The $\nu(COO^-)$ vibrations shift to lower frequencies ($\Delta\nu$ = 40–70 cm^{-1}) after the metallic ion coordinating to the oxygen atom of the carbonyl group [15]. In the IR spectra of precursor (P_2), the $\nu(COO^-)$ vibration locates at 1422 cm^{-1}. But in the IR spectra of the hybrid material (Tb-M_2), the $\nu(COO^-)$ vibration shifts to the 1384 cm^{-1}. The shift is a proof for the coordination effect between the carboxylic group and the metallic ion.

The UV absorption spectra of 4-mercaptobenzoic acid (T) and two precursors (P_1–P_4) are shown in Fig. 3. The absorption bands corresponded to the $\pi \rightarrow \pi^*$ electronic transition in the curve of T and two precursors located at 274, 254 nm, respectively. It is obvious that a blue shift of the major $\pi \rightarrow \pi^*$ electronic transition occurs. So it is estimated that during the modification of 4-mercaptobenzoic acid, the change of the group connected to the phencynonate increases the energy difference levels among electron transitions. In the UV absorption spectra of P_1, the absorption peak corresponded to the $n \rightarrow \pi^*$ electronic transition (R strip) locates at 290 nm. This can be attributed to the residual S_1 in the P_1 components. The wide absorption bands in the ultraviolet region of these two precursors are favorable for the effective intramolecular energy migration.

The selected XRD patterns of the two europium hybrid materials in Fig. 4 reveal that they are totally amorphous with range of $10° \leq n \leq 70°$. These broad signals correspond to the existence of a short-range order in the material [35]. These broad signals in two curves centered on 23° in the XRD patterns because of the coherent diffraction of the siliceous backbone in the hybrids [36,37]. The absence of any crystalline regions in these samples correlates well with the presence of organic chains in the host inorganic framework. It can be concluded that neither pure crystalline 4-

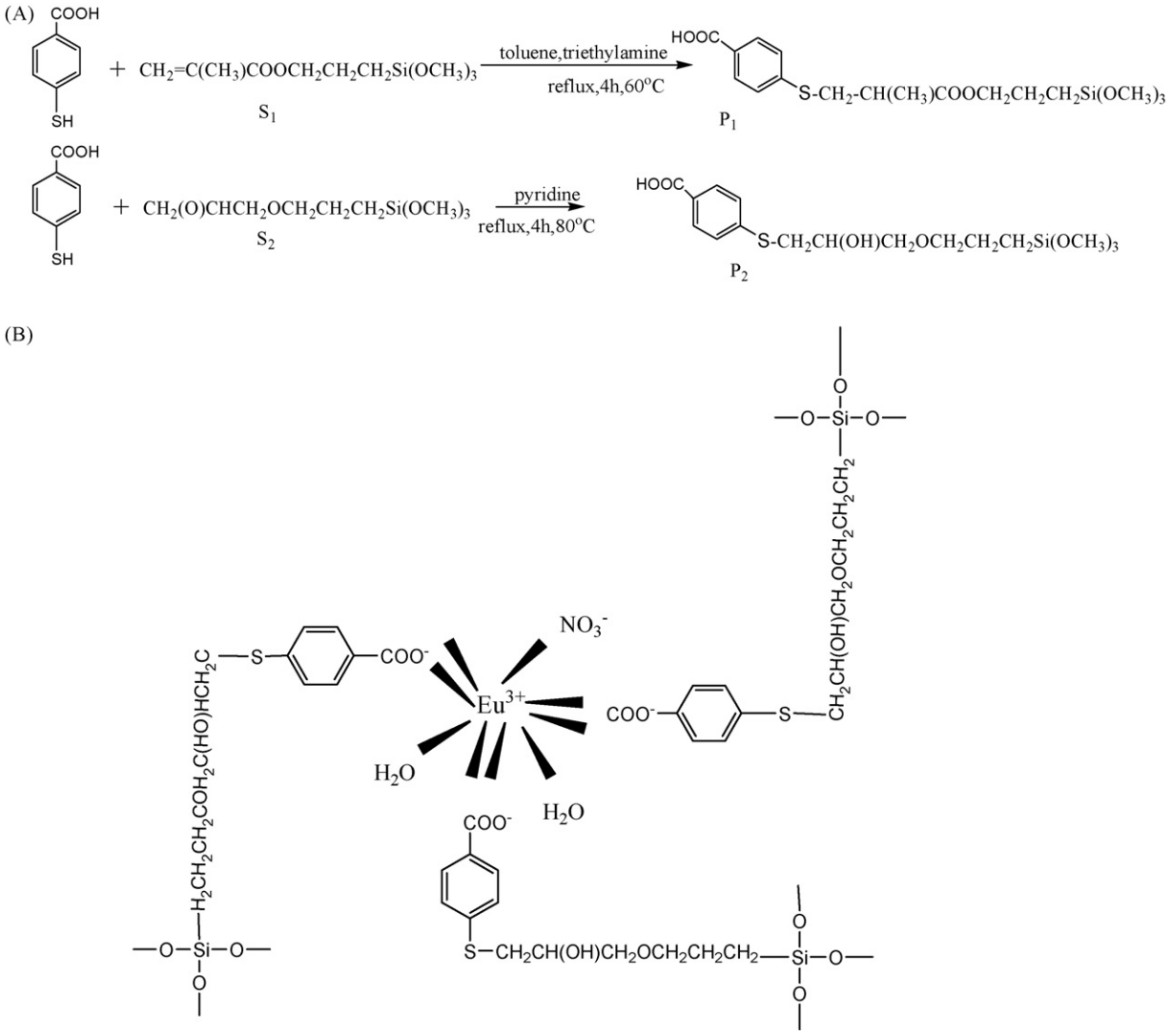

Fig. 1. Scheme for synthesis of two precursors (A) from the modification of 4-mercaptobenzoic acid and the selected predicted composition of Eu-M_2 (B).

mercaptobenzoic acid nor crystalline lanthanide complexes occur throughout the range of these hybrids.

Fig. 5 shows the selected UV–vis DRS curves of Eu-M_1, Tb-M_1 hybrids, which both have broad absorption band ranging from 200 to 480 nm. This suggests that the organic part plays an important role in the energy absorption process. The negative absorption peak corresponding to the characteristic emission peak at 614 nm of the active europium ions can be observed in the spectrum of Eu-M_1 hybrids. These negative absorption peaks are due to the $^5D_0 \rightarrow {}^7F_2$ transitions of the Eu^{3+} ion excited by the UV component in the incident ray during the measurement. The spectrum of Tb-M_1 hybrids shows that the negative absorption peak is the characteristic emission peak at 545 nm of the active terbium ions.

Fig. 6 illustrates typical photoluminescence spectra of the europium hybrid materials. All these emission spectra exhibit that the emission consisting of the $^5D_0 \rightarrow {}^7F_1$, $^5D_0 \rightarrow {}^7F_2$ transitions at 590 and 613 nm, respectively, while the emission lines of $^5D_0 \rightarrow {}^7F_3$ and $^5D_0 \rightarrow {}^7F_4$ are too weak to be observed. The $^5D_0 \rightarrow {}^7F_2$ emission around 613 nm is the most predominant transition, which agrees with the amorphous characters of the hybrid materials. Besides, there exists apparent emission in the short wavelength region at around 550 nm, which may be ascribed to the emission of the ligand. This phenomenon shows that the intramolecular energy transfer between the ligand and the europium ions is not so efficient because the triplet state energy of ligand is not suitable for the luminescence of europium ion.

Fig. 7 illustrates typical photoluminescence spectra of the terbium hybrid materials. The emission lines are assigned to the $^5D_4 \rightarrow {}^7F_J$ transitions located at 487, 542, 581 and 619 nm, for $J = 6, 5, 4, 3$, respectively. Among these emission peaks, the most striking green luminescence ($^5D_4 \rightarrow {}^7F_5$) and blue luminescence ($^5D_4 \rightarrow {}^7F_6$) indicated that the effective energy transfer took place between the ligand and the chelated Tb^{3+} ions. The green emission is stronger than that of the blue one. The reason may be that the emission to $^5D_4 \rightarrow {}^7F_6$ is an electronic dipole transition, which is greatly influenced by the ligand field. While the emission to $^5D_4 \rightarrow {}^7F_5$ belongs to a magnetic dipole transition and is less influenced by the ligand field. Besides, these bands due to the emission of the ligand cannot be clearly found in the spectra of terbium hybrid materials, suggesting that there exist more effective energy transfer process in the terbium hybrids than europium ones.

Fig. 8 shows the selected emission spectra of the zinc hybrid materials. The luminescence principle of zinc hybrids is different from that of lanthanide molecular hybrids. The luminescence of Lanthanide molecular hybrids are based on the intramolecular energy transfer between ligand and Ln^{3+}, but the luminescence of zinc molecular hybrid systems derives from the ligands influenced

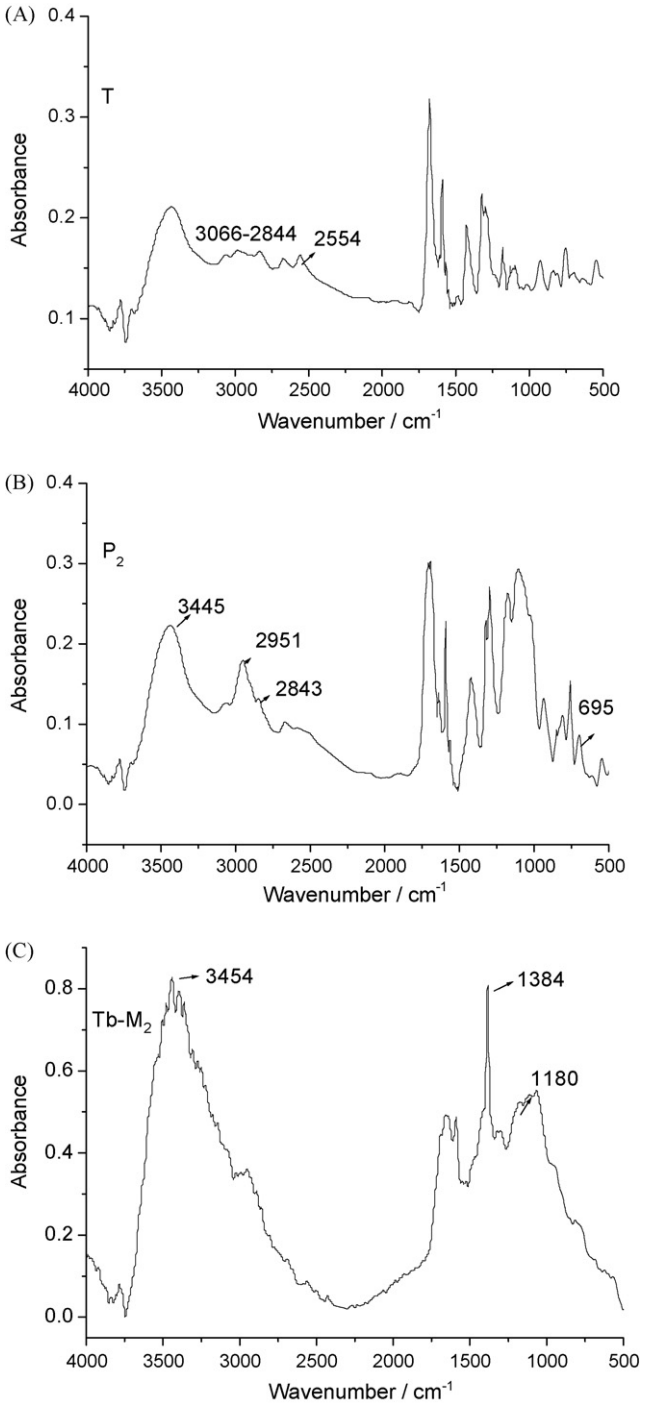

Fig. 2. FTIR spectra for 4-mercaptobenzoic acid (T), P_2 and Tb-M_2.

by the disturbance of Zn^{2+}. The wide emission peaks of both zinc hybrids are located at the range of 450–500 nm.

The typical decay curve of these two Eu^{3+} hybrid materials are measured and they can be described as a single exponential ($\mathrm{Ln}(S(t)/S_0) = -k_1 t = -t/\tau$), indicating that all Eu^{3+} ions occupy the same average coordination environment. The resulting lifetime data of Eu^{3+} hybrid materials are given in Table 1. We selectively determine the emission quantum efficiencies of the $^5D_0$ excited state of europium ion for Eu^{3+} hybrids on the basis of the emission spectra and lifetimes of the $^5D_0$ emitting level, the detailed luminescent data are shown in Table 1. The quantum efficiency of the luminescence step, η expresses how well the radiative processes

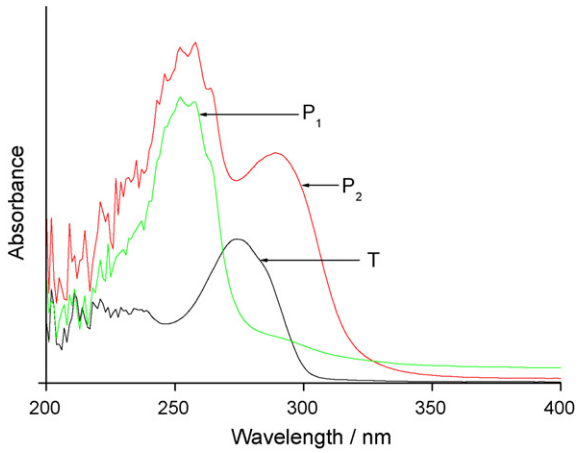

Fig. 3. Ultraviolet absorption spectra of 2-mercaptonicotinic acid (T) and two precursors ($P_{1,2}$).

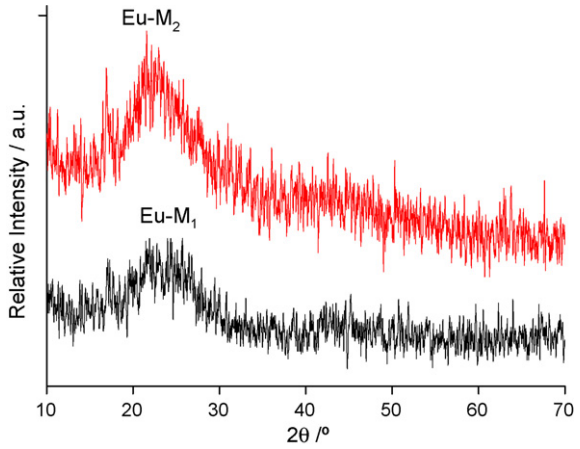

Fig. 4. X-ray diffraction (XRD) graphs of the hybrid material Eu(Zn)-$M_{1,2}$.

(characterized by rate constant A_r) compete with non-radiative processes (overall rate constant A_{nr}) [38–40].

$$\eta = \frac{A_r}{A_r + A_{nr}} \quad (1)$$

So quantum efficiency can be calculated from radiative transition rate constant (A_r) and experimental luminescence lifetime.

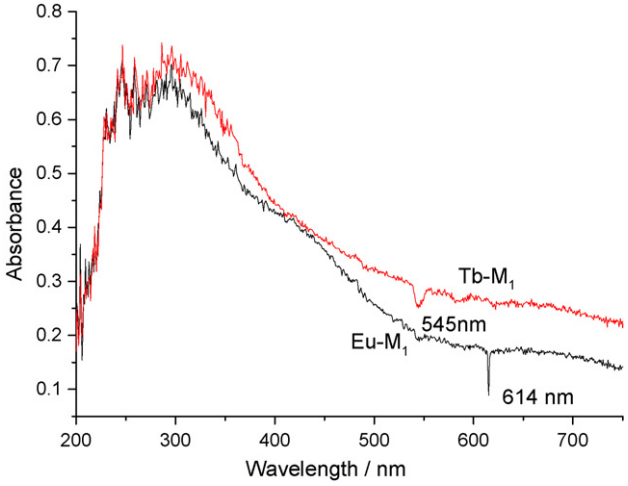

Fig. 5. UV–vis DRS spectra of Eu-M_1 and Tb-M_1.

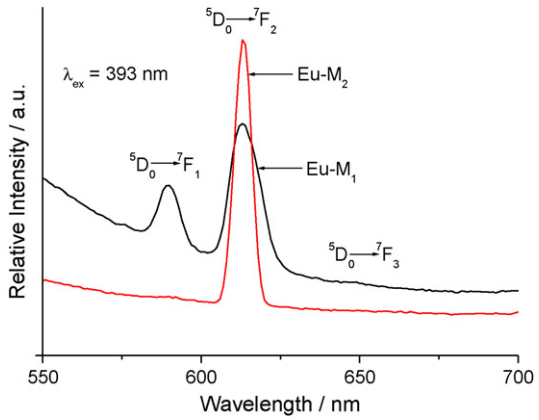

Fig. 6. Emission spectra of europium hybrid materials.

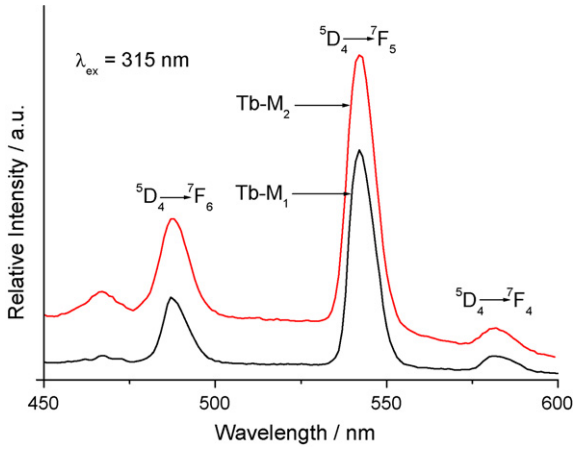

Fig. 7. Emission spectra of terbium hybrid materials.

Among A_r can be obtained by summarizing over the radiative rates A_{0J} for each $^5D_0 \rightarrow ^7F_J$ transitions of Eu^{3+}. Since $^5D_0 \rightarrow ^7F_1$ belongs to the isolated magnetic dipole transition, it is practically independent of the chemical environments around the Eu^{3+} ion, and thus can be considered as an internal reference for the whole spectrum, the experimental coefficients of spontaneous emission (A_{0J}) can be calculated. On the basis of the above discussion, the quantum efficiencies of these two kinds of europium hybrid materials can be calculated and the related data and the result are given in Table 1.The quantum efficiencies of the two kinds of europium complex hybrid materials can be determined in the following order:

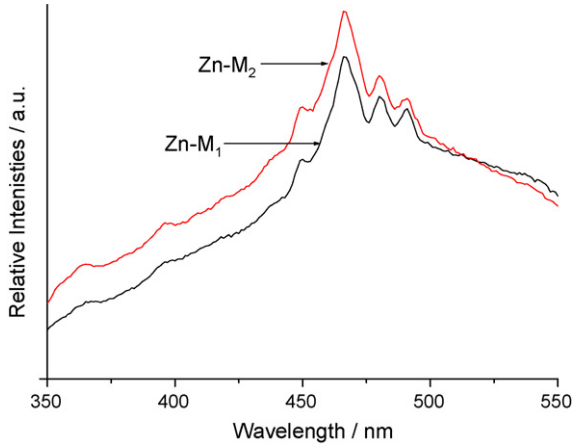

Fig. 8. Emission spectra of zinc hybrid materials.

Table 1
The luminescence efficiencies and lifetimes of the europium covalent bonded hybrids.

Systems	Eu-M_1	Eu-M_2
τ (ms)	0.60	0.50
υ_{01} (cm^{-1})[a]	16,978	16,926
υ_{02} (cm^{-1})[a]	16,308	16,304
υ_{03} (cm^{-1})[a]	15,413	15,327
υ_{04} (cm^{-1})[a]	14,936	14,316
I_{01}[b]	122.3	43.3
I_{02}[b]	167.7	226.4
I_{03}[b]	53.5	33.0
I_{04}[b]	47.9	30.6
A_{01} (s^{-1})	50	50
A_{02} (s^{-1})	71.4	271.7
A_{03} (s^{-1})	24.1	42.1
A_{04} (s^{-1})	22.3	41.8
A_{rad} (s^{-1})	167.8	405.6
η (%)	10.1	20.3

[a] The energies of the $^5D_0 \rightarrow ^7F_J$ transitions (υ_{0J}).
[b] The integrated intensity of the $^5D_0 \rightarrow ^7F_J$ emission curves.

Eu-M_2 > Eu-M_1, which are not in agreement with the order of lifetimes. This disagreement can be due to the influence of red/orange ratio (I_{02}/I_{01}). The red/orange ratio of the Eu-M_2 is much higher than the other three materials, and this made the quantum efficiencies of Eu-M_2 the highest when the lifetimes are similar. From the equation of η, it can be seen the value η mainly depends on the values of two quantum: lifetimes and red/orange ratio (I_{02}/I_{01}). If the lifetimes and red/orange ratio are large, the quantum efficiency must be high. The different composition of the hybrid materials may have influence on the luminescent lifetimes and quantum efficiencies.

4. Conclusions

In summary, a new series of luminescent chemically bonded lanthanide (and zinc) hybrid materials have been achieved using the 4-mercaptobenzoic acid derivative precursors. The different functional molecular bridges have some influence on the photophysical properties such as luminescent lifetimes and quantum efficiencies. So this kind of molecular-based hybrid material can be expected to be a promising candidate for tailoring desired properties to the host in many fields of applications.

Acknowledgements

This work is supported by the National Natural Science Foundation of China (20971100) and Program for New Century Excellent Talents in University (NCET-08-0398).

References

[1] G. Ramos, T. Belenguer, D. Levy, Highly photoconductive poly (vinylcarbazole)/2,4,7-trinitro-9-fluorenone sol–gel material that follows a classical charge-generation model, J. Phys. Chem. B 110 (2006) 24780–24785.
[2] P.N. Minoofar, R. Hernandez, S. Chia, B. Dunn, J.I. Zink, A.C. Franville, Placement and characterization of pairs of luminescent molecules in spatially separated regions of nanostructured thin films, J. Am. Chem. Soc. 124 (2002) 14388–14396.
[3] L. Zhao, D.A. Loy, K.J. Shea, Photodeformable spherical hybrid nanoparticles, J. Am. Chem. Soc. 128 (2006) 14250–14251.
[4] J.A. Chaker, C.V. Santilli, S.H. Pulcinelli, K. Dahmouche, V. Briois, P. Judeinstein, Multi-scale structural description of siloxane-PPO hybrid ionic conductors doped by sodium salts, J. Mater. Chem. 17 (2007) 744–757.
[5] C. Sanchez, G.J. de, A.A. Sloer-Illia, F. Ribot, T. Lalot, C.R. Mayer, V. Cabuil, Designed hybrid organic–inorganic nanocomposites from functional nanobuilding blocks, Chem. Mater. 13 (2001) 3061–3083.
[6] L.R. Matthews, E.T. Knobbe, Luminescence behavior of europium complexes in sol–gel derived host materials, Chem. Mater. 5 (1993) 1697–1700.
[7] B. Lebeau, C.E. Fowler, S.R. Hall, Transparent thin films and monoliths prepared from dye-functionalized ordered silica mesostructures, J. Mater. Chem. 9 (1999) 2279–2281.

[8] P. Innocenzi, H. Kozuka, T.J. Yoko, Fluorescence properties of the Ru(bpy)(3)(2+) complex incorporated in sol–gel-derived silica coating films, J. Phys. Chem. B 101 (1997) 2285–2291.
[9] B. Yan, H.J. Zhang, J.Z. Ni, Luminescence properties of the rare earth (Eu^{3+} and Tb^{3+}) complexes with 1,10-phenanthroline incorporated in silica matrix by a sol–gel method, Mater. Sci. Eng. B52 (1998) 123–128.
[10] O.A. Serra, E.J. Nassar, I.L.V. Rosa, Tb^{3+} molecular photonic devices supported on silica gel and functionalized silica gel, J. Lumin. 72–74 (1997) 263–265.
[11] M. Bredol, U. Kynast, M. Boldhaus, C. Lau, Luminescent inorganic networks, Ber. Bunsen-Ges. Phys. Chem. Chem. Phys. 102 (1998) 1557–1660.
[12] C. Sanchez, F. Ribot, Design of hybrid organic–inorganic materials synthesized via sol–gel chemistry, New J. Chem. 18 (1994) 1007–1037.
[13] L.D. Carlos, R.A.S. Ferreira, V.D. Bermudez, J.L.S. Ribeiro, Lanthanide-containing light-emitting organic–inorganic hybrids: A bet on the future, Adv. Mater. 21 (2009) 509–534.
[14] K. Binnemans, Lanthanide-based luminescent hybrid materials, Chem. Rev. 109 (2009) 4283–4374.
[15] A.C. Franville, D. Zambon, R. Mahiou, Y. Troin, Luminescence behavior of sol-gel-derived hybrid materials resulting from covalent grafting of a chromophore unit to different organically modified alkoxysilanes, Chem. Mater. 12 (2000) 428–435.
[16] H.R. Li, J. Lin, H.J. Zhang, H.C. Li, L.S. Fu, Q.G. Meng, Novel covalently bonded hybrid materials of europium (terbium) complexes with silica, Chem. Commun. (2001) 1212–1213.
[17] H.R. Li, J. Lin, H.J. Zhang, L.S. Fu, Q.G. Meng, S.B. Wang, Preparation and luminescence properties of hybrid materials containing europium(III) complexes covalently bonded to a silica matrix, Chem. Mater. 14 (2002) 3651–3655.
[18] M.C. Goncalves, V.D. Bermudez, R.A.S. Ferreira, L.D. Carlos, D. Ostrovskii, J. Rocha, Optically functional di-urethanesil nanohybrids containing Eu^{3+} ions, Chem. Mater. 16 (2004) 2530–2543.
[19] L.D. Carlos, R.A.S. Ferreira, R.N. Pereira, M. Assuncao, V.D. Bermudez, White-light emission of amine-functionalized organic/inorganic hybrids: emitting centers and recombination mechanisms, J. Phys. Chem. B 108 (2004) 14924–14932.
[20] Q.M. Wang, B. Yan, Novel luminescent terbium molecular-based hybrids with modified meta aminobenzoic acid covalently bonded with silica, J. Mater. Chem. 14 (2004) 2450–2455.
[21] Q.M. Wang, B. Yan, Molecular assembly of red and green nanophosphors from amine-functionalized covalent linking hybrids with emitting centers of Eu^{3+} and Tb^{3+} ions, J. Photochem. Photobiol. A: Chem. 178 (2006) 70–75.
[22] Q.M. Wang, B. Yan, A novel way to luminescent terbium molecular-scale hybrid materials: modified heterocyclic ligands covalently bonded with silica, Cryst. Growth Des. 5 (2006) 497–503.
[23] Q.M. Wang, B. Yan, Construction of lanthanide luminescent molecular-based hybrid material using modified functional bridge chemically bonded with silica, J. Photochem. Photobiol. A: Chem. 175 (2005) 159–165.
[24] Q.M. Wang, B. Yan, Terbium/zinc luminescent hybrid siloxane-oxide materials bridged by novel ureasils linkages, J. Organomet. Chem. 691 (2006) 540–545.
[25] J.L. Liu, B. Yan, Lanthanide (Eu^{3+}, Tb^{3+}) centered hybrid materials using modified functional bridge chemical bonded with silica: molecular design, physical characterization and photophysical properties, J. Phys. Chem. B 112 (2008) 10898–10907.
[26] H.F. Lu, B. Yan, J.L. Liu, Functionalization of calix[4]arene as molecular bridge to assemble novel luminescent lanthanide supramolecular hybrid systems, Inorg. Chem. 48 (2009) 3966–3975.
[27] H.F. Lu, B. Yan, Attractive sulfonamide bridging bonds constructing lanthanide centered photoactive covalent hybrids, J. Non-cryst. Solids 352 (2006) 5331–5336.
[28] B. Yan, Q.M. Wang, First two luminescent molecular hybrids composed of bridged Eu(III)-β-diketone chelates covalently trapped in silica and titanate gels, Cryst. Growth Des. 6 (2008) 1484–1489.
[29] S. Vijaikumar, K. Pitchumani, Simple, solvent free syntheses of unsymmetrical sulfides from thiols and alkyl halides using hydrotalcite clays, J. Mol. Catal. A: Chem. 217 (2004) 117–120.
[30] M. Bandini, P.G. Cozzi, M. Giacomini, P. Melchiorre, A. Umani-Ronchi, InBr3-catalyzed friedel-crafts addition of indoles to chiral aromatic epoxides: a facile route to enantiopure indolyl derivatives, J. Org. Chem. 67 (2002) 5386–5389.
[31] B. Yan, H.F. Lu, Lanthanide centered covalently bonded hybrids through sulfide linkage: molecular assembly, physical characterization and photoluminescence, Inorg. Chem. 47 (2008) 5601–5611.
[32] B. Yan, K. Qian, H.F. Lu, Chemically bonded metallic (Eu, Tb, Zn) hybrid materials through sulfide linkage: molecular construction, physical characterization and photophysical properties, J. Organomet. Chem. 694 (2009) 3160–3166.
[33] P.P. Lima, S.A. Junior, O.L. Malta, L.D. Carlos, R.A.S. Ferreira, R. Pavithran, M.L.P. Reddy, Synthesis, characterization, and luminescence, properties of Eu^{3+} 3-phenyl-4-(4-toluoyl)-5-isoxazolonate based organic–inorganic hybrids, Eur. J. Inorg. Chem. (2006) 3923–3929.
[34] D.D. Perrin, W.L.F. Armarego, D.R. Perrin, Purification of Laboratory Chemicals, Pergamon Press, Oxford, 1980.
[35] G. Cerveau, R.J.P. Corriu, E. Framery, F. Lerouge, Auto-organization of nanostructured organic–inorganic hybrid xerogels prepared by sol–gel processing: the case of a "twisted" allenic precursor, Chem. Mater. 16 (2004) 3794–3799.
[36] R.A.S. Ferreira, L.D. Carlos, R.R. Goncalves, S.J.L. Ribeiro, V.D. Bermudez, Energy-transfer mechanisms and emission quantum yields In Eu^{3+}-based siloxane-poly(oxyethylene) nanohybrids, Chem. Mater. 13 (2001) 2991–2998.
[37] S.S. Nobre, P.P. Lima, L. Mafra, R.A.S. Ferreira, R.O. Freire, L.S. Fu, U. Pischel, V.D. Bermudez, O.L. Malta, L.D. Carlos, Energy transfer and emission quantum yields of organic–inorganic hybrids lacking metal activator centers, J. Phys. Chem. C 111 (2007) 3275–3284.
[38] M.H.V. Werts, R.T.F. Jukes, J.W. Verhoeven, The emission spectrum and the radiative lifetime of Eu^{3+} in luminescent lanthanide complexes, Phys. Chem. Chem. Phys. 4 (2002) 1542–1548.
[39] E.E.S. Teotonio, J.G.P. Espynola, H.F. Brito, O.L. Malta, S.F. Oliveria, D.L.A. de Foria, C.M.S. Izumi, Influence of the N-[methylpyridyl]acetamide ligands on the photoluminescent properties of Eu(III)-perchlorate complexes, Polyhedron 21 (2002) 1837–1844.
[40] O.L. Malta, H.F. Brito, J.F.S. Menezes, F.R. Goncalves e Silva, S. Alves, F.S. Farias, A.V.M. Andrade, Spectroscopic properties of a new light-converting device Eu(thenoyltrifluoroacetonate), 2(dibenzyl sulfoxide). A theoretical analysis based on structural data obtained from a sparkle model, J. Lumin. 75 (1997) 255–268.